Shubnikov-de Haas effect study of cylindrical Fermi surfaces in UAs_2

2000 J. Phys.: Condens. Matter 12 1971

(http://iopscience.iop.org/0953-8984/12/9/302)

J. Phys.: Condens. Matter **12** (2000) 1971–1980. Printed in the UK PII: S0953-8984(00)07685-2

Shubnikov–de Haas effect study of cylindrical Fermi surfaces in UAs_2

P Wiśniewski†‖, D Aoki†, N Watanabe†, K Miyake†, R Settai†, Y Ōnuki†, Y Haga‡, E Yamamoto‡ and Z Henkie§

† Graduate School of Science, Osaka University, Toyonaka, Osaka 560-0043, Japan
‡ Advanced Science Research Centre, JAERI, Tokai, Ibaraki 319-1195, Japan
§ Institute for Low Temperatures and Structure Research, Polish Academy of Sciences, PO Box 1410, 50-950 Wrocław 2, Poland

Received 10 September 1999, in final form 15 December 1999

Abstract. Shubnikov–de Haas effect measurements were performed on a high-quality whisker single crystal of UAs_2. Complementary electrical resistivity and specific heat experiments were also carried out. Five of the seven detected branches exhibit angular dependences clearly indicating cylindrical Fermi surfaces. The effective cyclotron masses were determined to range from 0.33 to 4.5 m_0, which yielded an electronic specific heat coefficient of 10 mJ K^{-2} mol^{-1}. This is in very good agreement with the value 11.7 mJ K^{-2} mol^{-1} determined directly by the low-temperature specific heat measurement. The two-dimensional Fermi surfaces are formed in a strongly flattened magnetic Brillouin zone and the conduction electrons are confined mainly in the U planes, indicating an important contribution of itinerant 5f electrons.

1. Introduction

UAs_2, like other uranium dipnictides, crystallizes in the anti-Cu_2Sb-type tetragonal structure (D^7_{4h} or $P/4nmm$ space group). All UX_2 (X = P, As, Sb and Bi) compounds order antiferromagnetically when the uranium atoms' magnetic moments parallel to the [001] direction form ferromagnetic (001) planes stacked along this direction in an antiferromagnetic ($\uparrow\downarrow\downarrow\uparrow$) sequence [1], as shown in figure 1. The same sequence appears in UP_2, UAs_2 and USb_2, whereas in UBi_2 it is ($\uparrow\downarrow\uparrow\downarrow$). The magnetic unit cell is in the first three compounds doubled along the [001] direction with respect to the chemical unit cell, bringing about a strongly flattened magnetic Brillouin zone. In UBi_2 the magnetic and chemical unit cells are identical.

The UX_2 series offers an interesting possibility of observation of an evolution of physical properties with increasing pnictogen-anion radius and, consequently, the interatomic distances directly modifying the hybridization of 5f electron states of uranium with the conduction band. Both the paramagnetic Curie temperature and the effective magnetic moment change monotonically with the pnictogen radius. On the other hand, neither the values of the ordered moment nor the ordering temperatures vary monotonically throughout the series. (T_N = 201, 273, 203, 183 K and μ_{ord} = 2.0, 1.61, 1.88, 2.1 μ_B, for X = P, As, Sb, Bi, respectively.) Such behaviour is ascribed to the combination of crystal-field and magnetic interaction [2].

‖ Author to whom any correspondence should be addressed.

0953-8984/00/091971+10$30.00

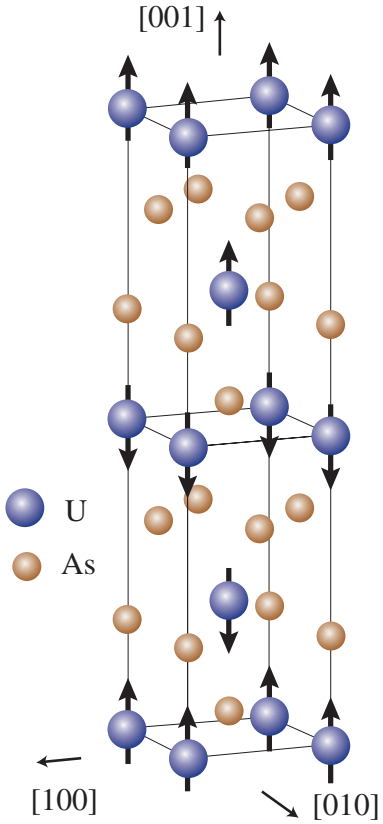

Figure 1. Crystal and magnetic structure of UAs_2.

Previous electron transport measurements on USb_2 [3] revealed a strong anisotropy of the electrical resistivity (ρ_c/ρ_a up to 160). Recent de Haas–van Alphen study [4] of the same compound clearly showed a quasi-two-dimensional character of the electronic structure (five cylindrical Fermi surfaces) with an important contribution from 5f electrons (the effective mass reaching 8.3 m_0).

In this work we present the results of Shubnikov–de Haas effect investigations, revealing the Fermi surface properties and the role of uranium 5f electrons in UAs_2.

Under a strong magnetic field, the orbital motion of conduction electrons is quantized and Landau levels are formed. When they cross the Fermi energy, as the magnetic field is changed, quantum oscillations occur in many physical properties. Measurement of these oscillations is a powerful method of determining the extremal cross-sectional area of the Fermi surface S_F, the effective cyclotron mass m^* and the relaxation time τ of the conduction electrons [5, 6]. Measurement of the magnetization and its field derivatives is the most common method for detecting the quantum oscillation, which is called the de Haas–van Alphen (dHvA) effect. When the oscillation appears in the magnetoresistance, it is called the Shubnikov–de Haas (SdH) effect. This method is particularly useful for small samples such as our whisker crystal.

2. Experiment

The single-crystal samples of UAs_2 were grown using the chemical transport method. Stoichiometric amounts of U and As were sealed in an evacuated quartz tube together with

3 mg cm^{-3} of iodine, serving as a transporting agent. After 100 hours of sintering at 750 °C, U and As fully reacted, forming polycrystalline UAs_2, which was then vapour transported for 20 days from the zone at 750 °C to the hotter zone at 900 °C. Numerous whisker-like single crystals have then grown on the walls of the ampoule. A sample with dimensions of $4 \times 0.2 \times 0.1$ mm^3 along the [100], [010] and [001] directions, respectively, was chosen for subsequent measurements.

The temperature dependence of the electrical resistivity ρ, measured by the conventional DC four-probe method with the current along the [100] direction, is shown in figure 2. The resistivity decreases steeply below 273 K, indicating the antiferromagnetic ordering. Below 8 K the resistivity shows Fermi liquid behaviour

$$\rho(T) = \rho(0) + aT^2$$

which is represented by a solid line in the inset of figure 2, where $\rho(0) = 0.29$ $\mu\Omega$ cm and $a = 1.97 \times 10^{-4}\mu\Omega$ cm K^{-2}. The high quality of the sample is confirmed by the residual resistivity ratio $\rho(280\text{ K})/\rho(0)$ of 580.

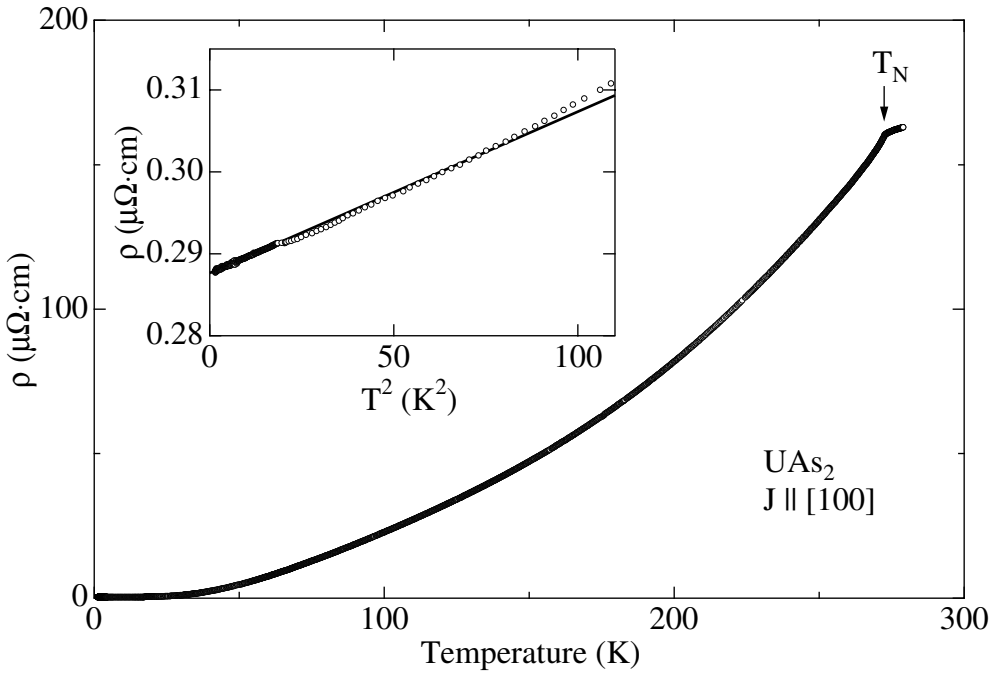

Figure 2. The temperature dependence of the electrical resistivity in UAs_2. The Fermi liquid behaviour at low temperatures is shown in the inset.

The SdH experiments were performed using both field-modulation and DC techniques, in magnetic fields up to 130 kOe and at temperatures down to 0.4 K. A four-probe configuration was used, with the direct current of 2 mA parallel to the [100] direction. In figure 3 the SdH oscillation observed using the field-modulation technique, in a magnetic field along [001] and ranging from 60 to 130 kOe, is shown together with the corresponding fast Fourier transform (FFT) spectrum. Similar spectra were obtained using the DC method. Seven fundamental branches were observed, labelled as α, β, γ, δ, ε, ζ and η, along with second harmonics 2ε, 2γ, and frequency-sum branches: $\delta+\varepsilon$, $\alpha+\varepsilon$, $\alpha+\delta$, $\alpha+\gamma$. The dHvA frequencies F ($=\hbar c S_F/2\pi e$) were small, ranging for fundamental branches from 3.9×10^6 to 4.3×10^7 Oe.

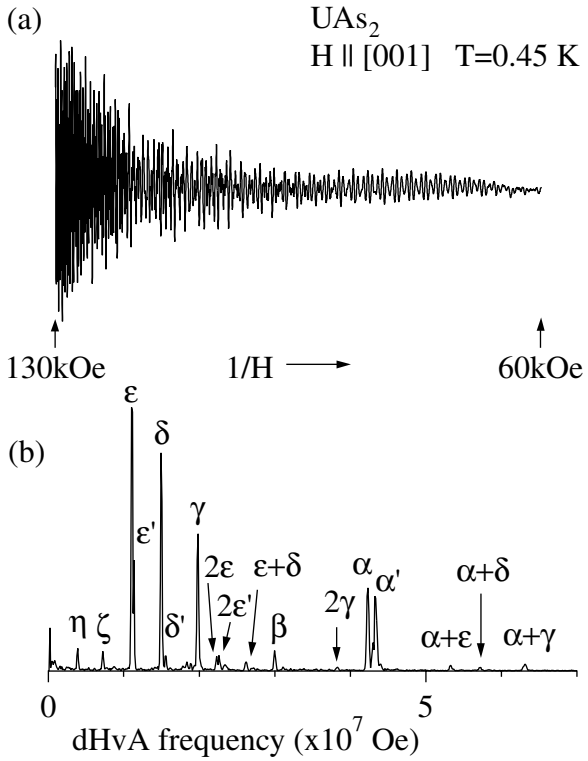

Figure 3. Shubnikov–de Haas oscillation for UAs_2 in a magnetic field along [001] (a) and the corresponding FFT spectrum (b).

The cylindrical form of the Fermi surfaces was derived from the angular dependence of the dHvA frequencies, displayed in figure 4, determined using the rotation of the sample, so the direction of the magnetic field was turned from [001] towards [100] by an angle θ. The frequencies of branches α, β, γ, δ and ε closely follow $1/\cos\theta$ dependences, shown by solid lines. Since the dHvA frequency is proportional to S_F, such dependence clearly indicates that all these branches correspond to cylindrical Fermi surfaces with axes along [001]. Branches β, ζ and η were, however, observed only in a narrow angular θ-region around [001]. Branch α is clearly split into two branches, α and α'. Most probably this means that the Fermi surface of branch α is not perfectly cylindrical but corrugated, possessing maxima and minima in cross-section. The branches δ and ε have similar properties.

Next, the effective cyclotron mass m^* was determined from the temperature dependence of the SdH amplitude, A, measured in a field ranging from 60 to 130 kOe. The results for all fundamental branches are shown as a so-called mass plot in figure 5. The fitting of linear functions to observed dependences yielded the effective cyclotron masses of 2.4(2), 4.5(7), 3.1(3), 2.1(1), 1.2(1), 0.34(08), 0.75(10) and 3.2(4) m_0 for branches α, β, γ, δ, ε, ζ, η and $\delta+\varepsilon$, respectively. The masses of other observed harmonic and frequency-sum branches could not be determined because of their small amplitudes.

We also determined how the amplitudes of the observed branches changed with the magnetic field. The linear fitting of the $\ln\{AH^{1/2}\sinh(\alpha m^*T/H)\}$ versus $1/H$ dependence

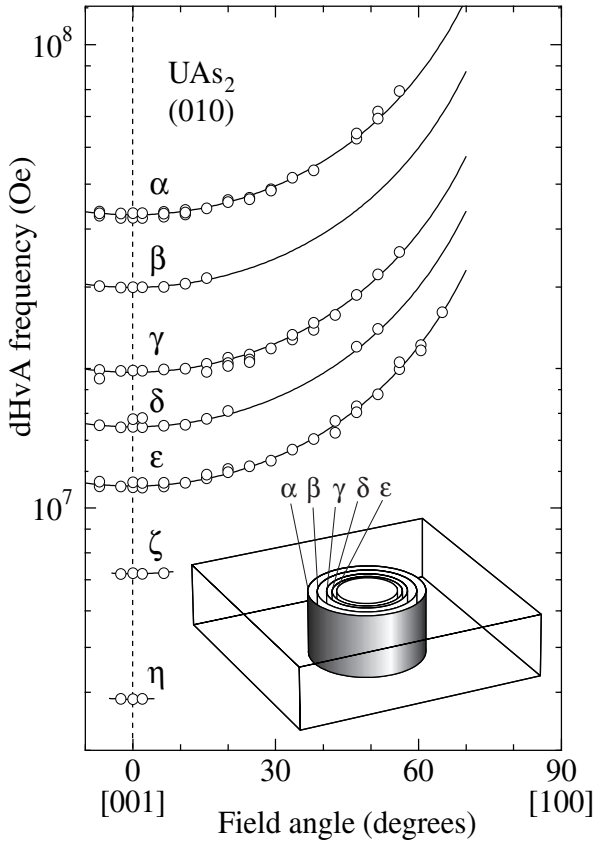

Figure 4. Angular dependences of the dHvA frequencies and, in the inset, a schematic diagram of the Fermi surface in UAs_2.

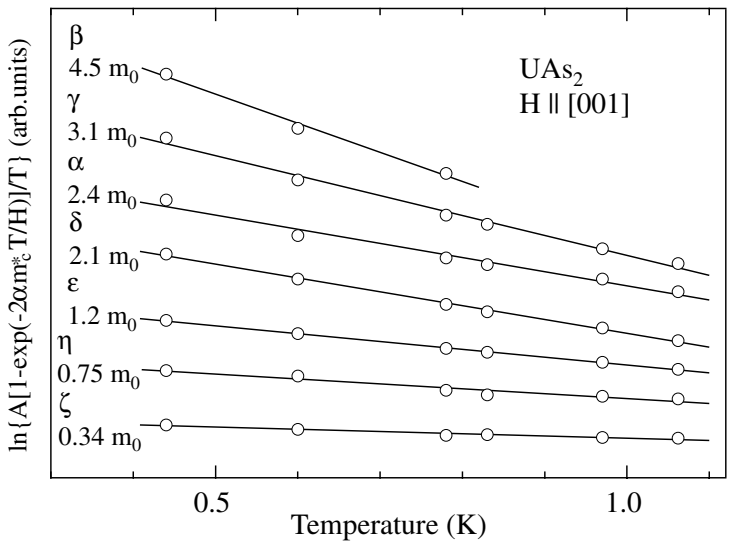

Figure 5. A mass plot for UAs_2.

(as described in [6]) gave values of the Dingle temperature T_D in the range from 1.4 to 8.6 K. From the simple relations $S_F = \pi {k_F}^2$, $\hbar k_F = m^* v_F$, $l = \hbar v_F \tau$ and $T_D = \hbar / 2\pi k_B \tau$, where k_F is half of the caliper dimension of S_F, we were able to estimate the mean free path l for all branches; it ranged from 660 Å to 1000 Å. The properties of the Fermi surface are summarized in table 1, together with those for USb_2 [4].

Table 1. The dHvA frequency F and effective cyclotron mass m^* for $\boldsymbol{H} \parallel [001]$, the Dingle temperature T_D and the mean free path l for UAs_2, along with F and m^* for USb_2 (from [4]).

	UAs_2				USb_2	
Branch	F (10^7 Oe)	m^* (m_0)	T_D (K)	l (Å)	F (10^7 Oe)	m^* (m_0)
α'	4.33	2.2				
α	4.23	2.4	3.2	660	3.86	4.2
β	3.00	4.5			2.80	8.3
γ	1.98	3.1	1.5	730	1.80	7.4
δ'	1.55	2.0				
δ	1.50	2.1	1.4	1000	1.22	4.0
ε'	1.14	1.1				
ε	1.11	1.2	2.3	910	0.76	1.8
ζ	0.72	0.34	8.6	720		
η	0.39	0.75	2.3	870		

The specific heat measurement was carried out on a polycrystalline sample (with the mass of 0.49 g) in the temperature range from 25 K down to 0.7 K. Figure 6 shows the results in the form of C/T versus T^2. At low temperatures, the specific heat can be expressed as

$$C/T = \gamma_S + bT^2.$$

The electronic specific heat coefficient γ_S was determined as 11.7 mJ K^{-2} mol^{-1}. This value is significantly different from the previously reported values of 45 mJ K^{-2} mol^{-1} [7] and

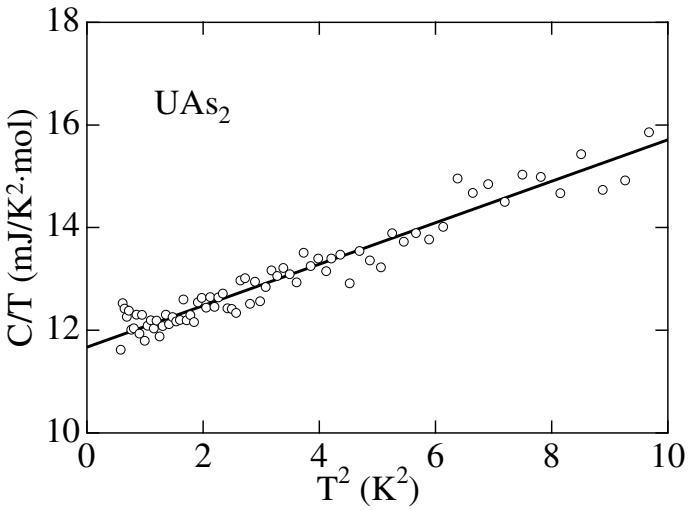

Figure 6. The specific heat of UAs_2 in the form of C/T versus T^2. A solid line represents the fit yielding the γ_S-value.

5.7 mJ K^{-2} mol^{-1} [8], which is understandable as the latter values were obtained from measurements performed at temperatures down to only 5 K. On the other hand, the value $\gamma_S = 11.7$ mJ K^{-2} mol^{-1} agrees very well with the value of 10 mJ K^{-2} mol^{-1} resulting from the effective cyclotron masses of five cylindrical Fermi surfaces (the surfaces ζ and η can be neglected because of their small volumes). The component of the electronic specific heat coefficient corresponding to the ith cylindrical Fermi surface (here $i = \alpha, \beta, \ldots, \varepsilon$) is proportional to the density of states at this surface:

$$\gamma_S^i = \frac{\pi^2 k_B^2}{3} \frac{\partial}{\partial E} \left(2 \frac{S(E) k_z}{V_{BZ}} \right) \Bigg|_{E=E_F}$$

where $S(E)$ is the cross-sectional area of the surface of constant energy E, k_z is the caliper dimension of the Brillouin zone in the [001] direction and V_{BZ} is the volume of the Brillouin zone. The total electronic specific heat coefficient can then be written as follows:

$$\gamma_S = \sum_i \gamma_S^i = \frac{k_B^2}{6\hbar^2} V k_z \sum_i m_i^*$$

where V denotes the volume of the unit cell.

3. Discussion

There is a possibility that observed branches with $F = 3.9 \times 10^6$ Oe and $F = 3.00 \times 10^7$ Oe are a $\delta - \varepsilon$ frequency-difference branch and a second harmonic of branch δ, respectively.

In the former case we believe that this is the fundamental branch, labelled η here, because its detected effective mass of 0.75 m_0 is much smaller than $m_\delta + m_\varepsilon = 3.3\ m_0$. The mass of the $\delta - \varepsilon$ branch due to the magnetic interaction should be equal to $m_\delta + m_\varepsilon$. On the other hand the detected mass of the clearly observed $\delta + \varepsilon$ frequency-sum branch $m_{\delta+\varepsilon} = 3.2\ m_0$ is almost equal to $m_\delta + m_\varepsilon$, which indicates the magnetic interaction as an origin of the $\delta + \varepsilon$ branch and the absence of magnetic breakdown between branches δ and ε (which could cause a discrepancy between $m_{\delta-\varepsilon}$ and $m_\delta + m_\varepsilon$). One can conclude, then, that the branch with $F = 3.9 \times 10^6$ Oe is most probably the fundamental one.

Since the amplitude of the dHvA oscillation A is proportional to a curvature factor $|\partial^2 S_F / \partial k_H^2|^{-1/2}$, where k_H denotes the component of the wave vector along the field direction [5, 6], the relatively wide angular range (up to over 50 degrees) over which the main branches were observed indicates a very large curvature factor, and consequently a rather simple form of the Fermi surface—most probably cylindrical surfaces with nearly circular cross-sections.

Tetragonal symmetry allows the cylindrical Fermi surfaces to be centred at only three points (and their symmetry equivalents) of the a^*b^*-plane in the reciprocal space: (0, 0), (0, $\frac{1}{2}$) and ($\frac{1}{2}$, $\frac{1}{2}$). The shortest distance between two such points is equal to a quarter of the reciprocal-space lattice constant: $\frac{1}{4}a^* = 3.97 \times 10^7$ cm^{-1}. For the biggest branch, α', the value $k_F = 3.62 \times 10^7$ cm^{-1}, calculated assuming a circular cross-section, is much smaller than $\frac{1}{4}a^*$. This means that even the biggest Fermi surfaces cannot cross each other, unless they have strongly curved (i.e. *not* circular) cross-sections.

Keeping in mind the complexity of the magnetic breakdown and the difficulty of distinguishing between the magnetic interaction and the magnetic breakdown on the basis of a limited set of experimental data and not very accurate values of the effective masses, we postulate that all harmonics and frequency-sum branches detected here are due to the magnetic interaction.

As regards the branch with $F = 3.00 \times 10^7$ Oe, despite its cyclotron mass (of 4.5 m_0) being close to $2m_\delta = 4.2\ m_0$, we postulate that it is not the branch 2δ but rather another

fundamental branch β, because a corresponding branch with $F = 2.80 \times 10^7$ Oe was found for USb_2 [4].

As far as the two-dimensionality of the Fermi surface is concerned, first of all it can be ascribed to the form of the magnetic unit cell which is elongated in the [001] direction. The corresponding Brillouin zone is small and flat, as shown schematically in the inset in figure 4. If a spherical Fermi surface exists in this Brillouin zone, its dHvA frequency should be smaller than 1.2×10^7 Oe. The frequencies of branches α, β, γ and δ, ranging from 1.5×10^7 Oe to 4.2×10^7 Oe, are larger than that.

The frequency of branch ε follows the $1/\cos\theta$ dependence up to 65°, indicating a cylindrical form of the corresponding Fermi surface. The forms of the Fermi surfaces of branches ζ and η are not clear, as they were observed only around the [001] direction and their frequencies are smaller than 1.2×10^7 Oe.

Another reason for the two-dimensionality of the Fermi surface is the sequence of the U and As planes, stacked along [001]. Recently, we observed cylindrical Fermi surfaces in CePtAs and CePtP [9], with the hexagonal crystal structures having a sequence of planes similar to that in UAs_2. In CePtAs the Pt and As atoms are in the same basal plane. The strong hybridization between the 5d electrons of Pt and 4p electrons of As in the Pt–As planes causes the quasi-two-dimensional character of the electronic band structure. The 4f electrons of Ce are fully localized and do not contribute to the conduction band. The effective cyclotron masses are therefore small, ranging from 0.47 to 0.84 m_0 for CePtAs and 0.34 to 0.80 m_0 for CePtP for magnitudes of the dHvA frequencies similar to those for UAs_2.

The cyclotron masses for UAs_2 as well as for USb_2 are, however, relatively large, so one can conclude that the 5f electrons become partially itinerant and are significantly contributing to the conduction band. It is also possible that their delocalization is stronger in the (001) plane than along the [001] direction, which would additionally strengthen the two-dimensionality of the Fermi surface. The conduction electrons are thus mainly 5f, 6d and 7s electrons in the U planes. It is thought that the conductive U planes are separated by the non-conductive As or Sb planes, which results in the two-dimensional Fermi surface.

γ_S for UAs_2 is equal to 11.7 mJ K^{-2} mol^{-1} (26 mJ K^{-2} mol^{-1} for USb_2). Correspondingly, the effective cyclotron masses for UAs_2 are almost half of the respective masses for USb_2, as shown in table 1. The distance between nearest-neighbour uranium atoms is larger in USb_2 (4.272 Å) than in UAs_2 (3.954 Å). The Néel temperature and the value of the ordered (effective) magnetic moment are 203 K and 1.88 μ_B/U (3.04 μ_B/U) for USb_2 and 273 K and 1.61 μ_B/U (2.94 μ_B/U) for UAs_2 [1,10,11]. These are natural trends, because the shorter the distance between nearest-neighbour U atoms, the more delocalized the 5f electrons become. The Pauli paramagnetic compounds UB_{12} and UB_2 are typical examples of an extreme case, where 5f electrons were shown to be itinerant by both the dHvA experiments and energy band calculations. In their case the detected cyclotron mass is equal to the calculated band mass [12–14].

The heavy-fermion systems such as $CeCu_6$, $CeRu_2Si_2$ and UPt_3 constitute another extreme case. Their magnetic susceptibilities increase with decreasing temperature, following the Curie–Weiss law, and have maxima at relatively low temperatures $T_{\chi_{max}}$. Below $T_{\chi_{max}}$ the susceptibilities become almost temperature independent and the character of the f-electron system changes from the localized to the itinerant heavy-fermion state via the many-body Kondo effect. For $CeCu_6$ and $CeRu_2Si_2$, $T_{\chi_{max}}$ corresponds approximately to the Kondo temperature T_K, which results in a large electronic specific heat coefficient γ_S ($\simeq 10^4/T_K$ (mJ mol^{-1} K^{-2})) [6, 15]. The enhanced low-temperature magnetic susceptibility χ_0 correlates with the large γ_S, following the Fermi liquid behaviour.

The mass enhancement is thus brought about by spin fluctuations, where the freedom of

the charge transfer of f electrons appears in the form of the f itinerant band, but the freedom of spin fluctuations of the same f electrons, revealed as the magnetic ordering, also enhances their effective mass. Although the Néel temperature for UAs_2 or USb_2 does not directly correspond to the characteristic temperature $T_{\chi_{max}}$, a value of the Néel temperature for UAs_2 larger than that for USb_2 is consistent with the above discussion. Both UAs_2 and USb_2 represent intermediate cases, located somewhere between the two above extremes. UAs_2, however, with its higher Néel temperature, resembles more closely the case of the above-mentioned Pauli paramagnets. This fact might crudely explain why the γ_S- and m^*-values for UAs_2 are smaller than those for USb_2.

Finally, we consider the volume of the Fermi surfaces shown in the inset in figure 4. Cylindrical Fermi surfaces corresponding to the branches α, β, γ, δ and ε occupy 16, 11, 7.5, 5.7 and 4.6% of the magnetic Brillouin zone, respectively. We neglect here the branches ζ and η because they have small volumes. As the magnetic unit cell of UAs_2 contains four molecules, this compound is a compensated metal with equal numbers of electron and hole carriers. The volume of branches α and δ is 22%, while that of branches β, γ and ε is 23% of the magnetic Brillouin zone. If we assume that the former two Fermi surfaces result from the electrons, the latter two should correspond to the holes.

Although one cannot expect an excellent agreement of calculated and measured effective masses, the band-structure calculations for UAs_2 certainly could confirm the electron or hole character of all detected Fermi surfaces and reveal their situation within the Brillouin zone (as they may not necessarily be centred at its origin, as shown in the inset of figure 4) as well as the details of the delocalization of the 5f electrons. Such calculations for all uranium dipnictide series are in progress.

In conclusion, cylindrical Fermi surfaces were observed in antiferromagnetic UAs_2. The two-dimensional character of these Fermi surfaces results from the strongly flattened magnetic Brillouin zone and the conduction electrons, including the itinerant 5f electrons, confined in the U planes.

Acknowledgments

This work was supported by the Grant-in-Aid for Scientific Research COE(10CE2004) from the Japan Ministry of Education, Science, Sports and Culture. D Aoki and P Wiśniewski acknowledge financial support from the Japan Society for the Promotion of Science in the frameworks of the *Research Fellowship for Young Scientists* and the *Postdoctoral Fellowship for Foreign Researchers*, respectively.

References

[1] Oleś A 1965 *J. Physique* **26** 561
[2] Amoretti G, Blaise A and Mulak J 1984 *J. Magn. Magn. Mater.* **42** 65
[3] Henkie Z, Maślanka R, Wiśniewski P, Fabrowski R, Markowski P J, Franse J J M and van Sprang M 1992 *J. Alloys Compounds* **181** 267
[4] Aoki D, Wiśniewski P, Miyake K, Watanabe N, Settai R, Yamamoto E, Haga Y and Ōnuki Y 1999 *J. Phys. Soc. Japan* **68** 2182
[5] Shoenberg D 1984 *Magnetic Oscillations in Metals* (Cambridge: Cambridge University Press)
[6] Ōnuki Y and Hasegawa A 1995 *Handbook on the Physics and Chemistry of Rare Earths* vol 20, ed K A Gschneidner Jr and L Eyring (Amsterdam: Elsevier) p 1
[7] Blaise A, Fournier J M, Langnier R, Mortimer M J, Schenkel R, Henkie Z and Wojakowski A 1978 *Rare Earths and Actinides 1977 (Inst. Phys. Conf. Ser. 37)* (Bristol: Institute of Physics Publishing) p 184
[8] Grønvold F, Zaki M R, Westrum E F Jr, Sommers J A and Downie D B 1978 *J. Inorg. Nucl. Chem.* **40** 635

[9] Settai R, Yoshida Y, Yamaguchi A, Ōnuki Y, Yoshii S, Kasaya M, Harima H and Takegahara K 1999 *J. Phys. Soc. Japan* **68** 3615
[10] Leciejewicz J, Troć R, Murasik A and Zygmunt A 1967 *Phys. Status Solidi* **22** 517
Leciejewicz J, Troć R, Murasik A and Zygmunt A 1967 *Phys. Status Solidi* **24** 763 (erratum)
[11] Trzebiatowski W, Sepichowska A and Zygmunt A 1964 *Bull. Acad. Pol. Sci. Ser. Chim.* **12** 687
[12] Yamagami Y and Hasegawa A 1991 *J. Phys. Soc. Japan* **60** 987
[13] Ōnuki Y, Umehara I, Kurosawa Y, Nagai N, Satoh K, Kasaya M and Iga F 1990 *J. Phys. Soc. Japan* **59** 2320
[14] Yamamoto E, Haga Y and Ōnuki Y 1998 *J. Phys. Soc. Japan* **67** 3171
[15] Besnus M J, Kappler J P, Lehmann P and Meyer A 1985 *Solid State Commun.* **55** 779